New Journal of Physics
The open access journal at the forefront of physics

Deutsche Physikalische Gesellschaft DPG IOP Institute of Physics

Spin-phonon coupling in antiferromagnetic chromium spinels

To cite this article: T Rudolf *et al* 2007 *New J. Phys.* **9** 76

New Journal of Physics
The open–access journal for physics

Spin-phonon coupling in antiferromagnetic chromium spinels

T Rudolf[1,3], Ch Kant[1], F Mayr[1], J Hemberger[1], V Tsurkan[1,2] and A Loidl[1]

[1] Experimental Physics V, Center for Electronic Correlations and Magnetism, University of Augsburg, D-86135 Augsburg, Germany
[2] Institute of Applied Physics, Academy of Sciences of Moldova, MD-2028 Chişinău, Republic of Moldova
E-mail: torsten.rudolf@physik.uni-augsburg.de

New Journal of Physics **9** (2007) 76
Received 21 December 2006
Published 27 March 2007
Online at http://www.njp.org/
doi:10.1088/1367-2630/9/3/076

Abstract. The temperature dependence of eigenfrequencies and intensities of the infrared (IR) active modes has been investigated for the antiferromagnetic chromium spinel compounds $CdCr_2O_4$, $ZnCr_2O_4$, $ZnCr_2S_4$, $ZnCr_2Se_4$, and $HgCr_2S_4$ by IR spectroscopy for temperatures from 5 to 300 K. At the transition into the magnetically ordered phases, and driven by spin-phonon coupling, most compounds reveal significant splittings of the phonon modes. This is true for geometrically frustrated $CdCr_2O_4$, and $ZnCr_2O_4$, for bond frustrated $ZnCr_2S_4$ and for $ZnCr_2Se_4$, which is also bond frustrated, but dominated by ferromagnetic (FM) exchange. The pattern of splitting is different for the different compounds and crucially depends on the nature of frustration and of the resulting spin order. $HgCr_2S_4$, which is almost FM, exhibits no splitting of the eigenfrequencies, but shows significant shifts due to FM spin fluctuations.

[3] Author to whom any correspondence should be addressed.

PII: S1367-2630(07)40237-3

Contents

1. Introduction 2
2. Experimental 5
3. Results and discussion 6
4. Conclusions 12
Acknowledgments 13
References 13

1. Introduction

It is known for more than 40 years that chromium spinels (ACr_2X_4) span an enormous range of magnetic exchange strengths and different magnetic ground states [1]. As a function of lattice constant, or equivalently as a function of Cr–Cr separation, these compounds are characterized by Curie–Weiss (CW) temperatures from −400 to 200 K and, at low temperatures, reveal either complex antiferromagnetism or ferromagnetism. The chromium oxide spinels undergo antiferromagnetic (AFM) ordering transitions of the order of 10 K, despite the fact that the exchange interactions, as deduced from the paramagnetic (PM) CW temperatures, are one order of magnitude larger. This can be explained by the fact that the Cr spins reside on a pyrochlore lattice revealing strong geometrical frustration. Some selenide spinels undergo ferromagnetic (FM) ordering at temperatures of the order of 100 K. The different ground states as a function of lattice constants are driven by the dominating exchange interactions: at small Cr–Cr separation strong direct AFM exchange dominates. With increasing separation the 90° FM Cr–X–Cr exchange becomes important. Probably for all lattice spacings a complex Cr–X–A–X–Cr super exchange (SE) is active. This AFM SE is weak and only of the order of 1 K, but gains importance via a high multiplicity [1].

In the spinel structure, Cr ions are located at the B-sites in an octahedral environment in a $3d^3$ state. Under the action of an octahedral crystal field the d levels split into a lower t_{2g} triplet, each orbital being singly occupied, and an excited empty e_g doublet. The resulting bulk material is a Mott insulator with $S = 3/2$, with an almost spherical charge distribution and negligible spin–orbit coupling. As a matter of fact, one can expect that in these compounds orbital effects are quenched, and that charge effects will play no role. The geometric frustration of the pyrochlore lattice and the bond frustration due to competing magnetic exchange [2] are responsible for emergent complex magnetic ground states [3], for strong metamagnetism [4, 5], and even for multiferroic behaviour [6, 7]. The complexity of the ground states becomes even more enhanced by the unconventional coupling of the spin-only chromium moments to the lattice. This has early been recognized on the basis of ultrasonic experiments on $ZnCr_2O_4$ by Kino and Lüthi [8] and later on, has been treated in modern theories on the basis of a spin-driven Jahn–Teller effect [9, 10].

Very recently, spin-phonon coupling in materials with strong electronic correlations gained considerable attention. Concerning the compounds under consideration, the onset of structural distortions and of AFM order in the geometrically frustrated oxides has been described using a concept in which the lattice distorts to gain exchange energy, and thereby relieves the frustration [9]–[11]. In $ZnCr_2S_4$, complex magnetic order results from strong bond-frustration characterized

Table 1. Lattice constants a_0(Å), fractional coordinate x, effective PM moment $p_{\text{eff}}(\mu_B)$, CW temperature Θ_{CW}(K), magnetic ordering temperature T_m(K) and magnetic frustration parameter $f = |\Theta_{CW}|/T_m$. The values documented in this table have, if not otherwise referenced, been taken from our own work, which mostly has been published [2], [4]–[7].

Compound		a_0	x	p_{eff}	Θ_{CW}	T_m	f
$ZnCr_2O_4$	ZCO	8.317(2)	0.265	3.85	−398	12.5	32
$MgCr_2O_4$	MCO	8.319(3)	0.261	3.71	−346	12.7	27
$CdCr_2O_4$	CCO	8.596(2)	0.265	4.03	−71	8.2	8.7
$HgCr_2O_4$	HCO	8.658(1)[a]	0.229[a]	3.72[b]	−32[b]	5.8[b]	5.5
$ZnCr_2S_4$	ZCS	9.983(2)	0.258	3.86	7.9	15; 8	0.5
$ZnCr_2Se_4$	ZCSe	10.498(2)	0.260	4.04	90	21	4.3
$HgCr_2S_4$	HCS	10.256(1)	0.267	3.90	140	22	6.4
$CdCr_2S_4$	CCS	10.247(2)	0.263	3.88	155	84.5	1.8
$CdCr_2Se_4$	CCSe	10.740(3)	0.264	3.82	184	130	1.4
$HgCr_2Se_4$	HCSe	10.737(3)	0.264	3.89	200	106	1.9

[a] Wessels *et al* [19].
[b] Ueda *et al* [20].

by FM and AFM exchange interactions of almost equal strength [2]. $ZnCr_2Se_4$ is dominated by FM exchange but orders antiferromagnetically at $T_N = 21$ K [12]. All these compounds show a strong splitting of specific phonon modes [2, 12, 13], which has been explained by *ab initio* approaches providing evidence that the dynamic anisotropy of the phonon modes is induced by the magnetic exchange interactions alone and can be fully decoupled from lattice distortions [14, 15]. The idea that magnetic exchange interactions and the onset of magnetic order strongly influence the phonon modes was outlined decades ago by Baltensperger and Helman [16, 17] and by Brüesch and D'Ambrogio [18].

In this paper, we report on detailed infrared (IR) experiments for a variety of spinels, ranging from compounds with strong geometric frustration to almost FM systems. We document spin-phonon coupling by splittings and significant shifts of different phonon modes, which are diverse for different spin orders. We try to correlate the shifts of the eigenfrequencies and the dynamic breaking of symmetry by the strength of competing exchange interactions. Table 1 shows room temperature lattice constants and fractional coordinates, PM moments, CW temperatures, magnetic ordering temperatures, and the magnetic frustration parameter $f = |\Theta_{CW}|/T_m$ for a number of chromium oxides, sulfides and selenides. From this table, it immediately becomes clear that with increasing lattice constant the CW temperatures increase from strongly negative AFM exchange in the oxides to moderately FM exchange in the selenides. As outlined above, in the oxides, AFM direct Cr–Cr exchange dominates all other exchange paths. With increasing lattice constant this direct exchange becomes considerably weaker and competes with 90° FM Cr–X–Cr exchange. Hg and Cd selenides are well known FM semiconductors with high FM ordering temperatures. At the same time, table 1 demonstrates that the chromium spins in the oxides exhibit strong geometrical frustration. In all compounds, the Cr moments are close to the spin-only values ($S = 3/2$, yielding 3.87 μ_B for the PM moment) demonstrating the absence of spin–orbit coupling.

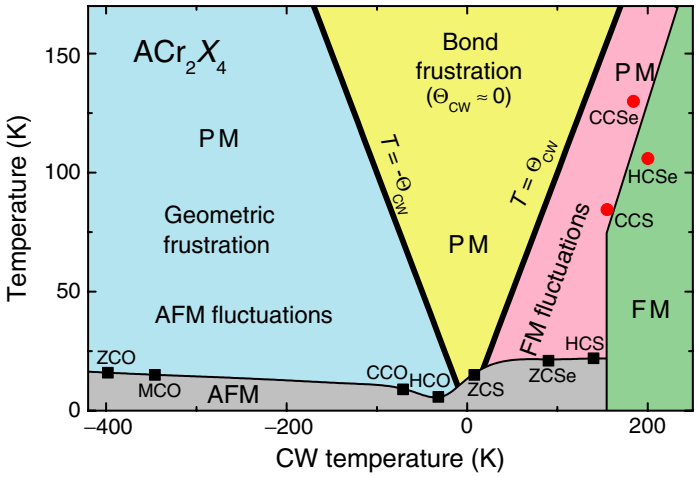

Figure 1. Schematic magnetic phase diagram of ACr_2X_4 compounds, where characteristic temperatures are plotted versus the CW temperature (see table 1): FM (red circles) and AFM (black squares) ordering temperatures. Hypothetical magnetic ordering temperatures ($T = \pm\Theta_{CW}$) are indicated by thick solid lines. Thin solid lines separate magnetically ordered from PM phases and are drawn to guide the eye.

The evolution of the magnetic properties of the chromium spinels is schematically shown in figure 1. Here we plot the characteristic ordering temperatures versus the CW temperatures. The CW temperatures scale with the lattice constants (see table 1), but, for presentation purposes we decided to take the CW temperatures as variables. In the complete regime from strongly negative CW temperatures (−400 K) to positive CW temperatures of almost 150 K, the ground states of all spinels exhibit antiferromagnetism with different spin arrangements: ZCO has a complex magnetic order with at least 64 spins per magnetic unit cell [3, 21]. CCO undergoes a magnetic phase transition into a phase with incommensurate spiral order, where a collinear state is twisted into a long spiral with the spins aligned in the *ac*-plane [21, 22]. In ZCS, FM and AFM exchange are almost of equal strength [2]. Consequently, the magnetic ground state is a mixed state, with the co-existence of a spiral and a collinear structure [23]. This mixed phase is established at 8 K. A magnetic precursor phase with a pure helical spin order appears at 15 K [23]. ZCSe and HCS are close to the FM border with CW temperatures of the order of 100 K. Both compounds are dominated by strong FM spin fluctuations but finally undergo AFM phase transitions with FM planes with a small turn angle of the spin directions of neighbouring planes [24]–[27]. Finally CCS, CCSe and HCSe are FM semiconductors with high ordering temperatures [1].

The oxides are dominated by strong direct AFM exchange. As the spins reside on a pyrochlore lattice, geometrical frustration suppresses conventional AFM order. The FM compounds are dominated by 90° nearest neighbour (nn) Cr–*X*–Cr exchange. In figure 1, the hypothetical FM and AFM ordering temperatures corresponding to the CW temperatures are indicated by thick solid lines. The temperature difference between this line and the real ordering temperature is a direct measure of the frustration of the system. The onset of AFM order is strongly reduced by geometrical frustration and in the low-temperature PM phase AFM fluctuations dominate the physics of these compounds. FM order becomes suppressed by the onset of competing AFM interactions and below the hypothetical ordering temperature FM

fluctuations control the low-temperature physics. In between these two lines with $T = -\Theta_{CW}$ and $T = \Theta_{CW}$, the PM regime extends to low temperatures because of bond frustration: here FM exchange and AFM Cr–X–A–X–Cr exchange, enhanced by residues of direct exchange, are of equal strength. It is important to note that even for a vanishing CW temperature local exchange interactions are still strong but compete and almost cancel each other out. In the cone between these two lines of expected magnetic order strong bond frustration is active, exemplified by the PM behaviour of ZCS, which reveals a CW temperature of almost 0 K and a mixed magnetic state at low temperatures [23]. Bond frustration still seems to be active for compounds with high FM CW temperatures, which exhibit antiferromagnetism at low temperatures. Finally, we would like to note that the spiral ground state in ZCSe has been explained assuming a set of five distinct distant–neighbour interactions [28].

A closer inspection of table 1 and figure 1 allows further deep insights into the dominating exchange paths: it is clear that the AFM exchange at small lattice constants, which is due to direct Cr–Cr overlap, becomes exponentially smaller with increasing lattice spacings. However, it remains unclear why the FM exchange strongly increases towards larger lattice constants. Table 1 shows that the lattice constants increase from 1.050 to 1.074 nm, when moving from ZCSe towards CCSe and HCSe, but the CW temperatures increase from 90 to 200 K and the FM ordering temperatures rise from 21 to 130 K. The low ordering temperature for the ZCSe can partly be explained by bond frustration, but it is hard to believe that AFM order via Cr–X–A–X–Cr depends so strongly on distance. The FM exchange should mainly depend on the Cr–X–Cr bond angle, which is 90° in the ideal spinel structure. This bond angle strongly depends on the fractional coordinate x [1]. From table 1 we conclude that, as x is almost constant for the ferromagnets under consideration, it cannot explain the difference in the FM exchange interactions, and one can speculate that the increase in FM exchange rather comes from an increasing covalency of the Cr–X–Cr bonds when moving from the sulfides to the selenides.

2. Experimental

Polycrystalline $CdCr_2O_4$, $ZnCr_2O_4$, $ZnCr_2S_4$, $ZnCr_2Se_4$, $HgCr_2S_4$ and $CdCr_2S_4$ samples were prepared by solid-state reaction from high-purity elements in evacuated quartz ampoules. The synthesis was repeated several times in order to reach good homogeneity. For the sulfides and selenides single crystals have also been grown by gas transport using chlorine as transport agent or by liquid-transport methods. Only the CCS and ZCSe samples were large enough to perform high precision optical experiments even at low wavenumbers. X-ray diffraction revealed cubic single-phase materials with lattice constants and anion fractional coordinates as indicated in table 1. Magnetic susceptibilities were measured with a commercial superconducting quantum interference device magnetometer for temperatures from 1.8 to 400 K. CW temperatures and PM moments are included in table 1. Reflectivity experiments were carried out in the far-IR range using the Bruker Fourier-transform spectrometer IFS113v equipped with a He bath cryostat. With our set-up of mirrors and detectors we were able to measure the frequency range from 50 to 700 cm^{-1}. The ceramic samples were pressed with a maximum pressure of 1 GPa. Nevertheless, neither the surface nor the density of the ceramics was ideal and of perfect optical quality. To correct for these factors we multiplied the measured reflectivities of the ceramic samples CCO, ZCO, ZCS and HCS by a factor of 1.2. This factor has been derived from a set of measurements of different sulfide- and selenide-spinels at room temperature in ceramic and single-crystalline

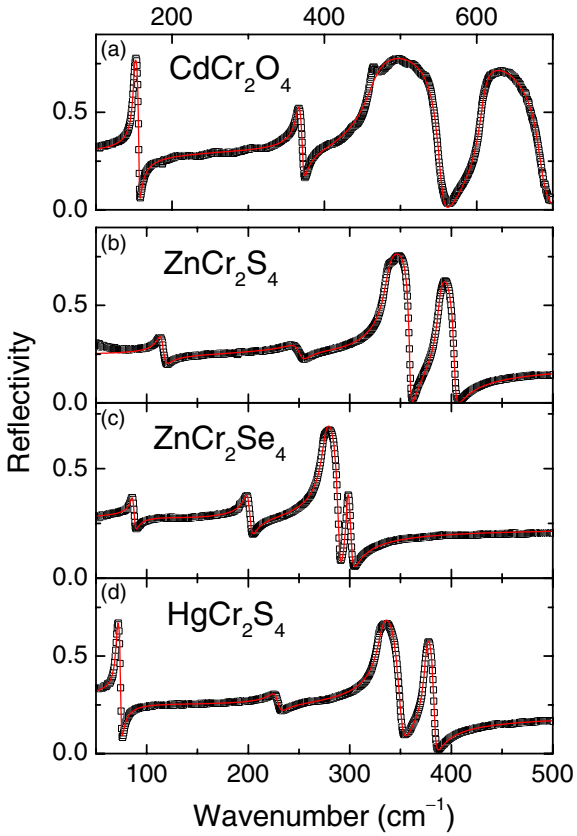

Figure 2. Room temperature reflectivity versus wavenumber for $CdCr_2O_4$ (a) $ZnCr_2S_4$ (b) $ZnCr_2Se_4$ (c) and $HgCr_2S_4$ (d). The solid lines represent the results of fits as described in the text. Please note the change of the wavenumber scale for frame (a).

form. The measurements on pressed ceramics hence limit the precision of the value of ϵ_∞ and concomitantly of the dielectric strength. But the absolute errors will be certainly less than 10% and will not affect the variation of the derived parameters as a function of temperature and external magnetic field.

3. Results and discussion

Reflectivity spectra as a function of temperature have been measured for all six compounds with AFM ground states. As expected from symmetry grounds, the spectra consist of four phonon triplets of F_{1u} symmetry. Figures 2(a)–(d) show the reflectivity spectra of $CdCr_2O_4$, $ZnCr_2S_4$, $ZnCr_2Se_4$ and $HgCr_2S_4$ at room temperature, which agree well with those previously measured [29, 30]. The small spikes in the reflectivity of $CdCr_2O_4$, which appear close to 440, 470 and 530 cm^{-1}, result from the surface roughness of the ceramic sample and show no temperature dependence. In the following, the four modes are labelled as mode 1 to 4 in ascending order from low to high wavenumbers.

To analyse the reflectivity spectra the complex dielectric function $\epsilon(\omega)$ was obtained by calculating the factorized form

$$\epsilon(\omega) = \epsilon_\infty \prod_j \frac{\omega_{\mathrm{L}j}^2 - \omega^2 - \mathrm{i}\gamma_{\mathrm{L}j}\omega}{\omega_{\mathrm{T}j}^2 - \omega^2 - \mathrm{i}\gamma_{\mathrm{T}j}\omega}. \tag{1}$$

Here $\omega_{\mathrm{L}j}$, $\omega_{\mathrm{T}j}$, $\gamma_{\mathrm{L}j}$ and $\gamma_{\mathrm{T}j}$ correspond to longitudinal (L) and transversal (T) eigenfrequency (ω_j) and damping (γ_j) of mode j, respectively. At normal incidence the dielectric function is related to the reflectivity via

$$R(\omega) = \left| \frac{\sqrt{\epsilon(\omega)} - 1}{\sqrt{\epsilon(\omega)} + 1} \right|^2. \tag{2}$$

From the measured reflectivity the values of ϵ_∞, $\omega_{\mathrm{L}j}$, $\omega_{\mathrm{T}j}$, $\gamma_{\mathrm{L}j}$ and $\gamma_{\mathrm{T}j}$ have been determined using a fit routine developed by Kuzmenko [31]. Results of these fits are shown for all reflectivity sets in figures 2(a)–(d). Despite the use of ceramic samples, the fit works very well. Only close to the maxima of mode 3, especially for CCO and ZCS, does the fit deviate slightly from the experimental data, probably resulting from a too low density and from surface imperfections of the ceramic samples.

Figure 3 shows the central result of this work, namely the temperature dependence of the eigenfrequencies of four different spinels: geometrically frustrated CCO, bond-frustrated ZCS, ZCSe, which is an AFM but already dominated by strong FM exchange, and finally HCS, which is almost FM. The latter two compounds reveal strong metamagnetic behaviour. A significant temperature dependence of the eigenfrequencies and a splitting of a number of modes below the magnetic ordering temperatures are clearly observable. Preliminary results on ZCS and ZCSe were published in [2, 12]. The phonon modes of ZCO have been investigated in detail in [13]. CCO, ZCS and ZCSe reveal very different splittings of the phonon modes in the AFM phase.

CCO exhibits a clear splitting of mode 2 and there are also indications of a splitting of mode 3. To exemplify these splittings of the phonon modes at the AFM transition of $CdCr_2O_4$, figure 4 shows the splitting of modes 2 and 3 in more detail on an enlarged scale for temperatures just above and below the magnetic ordering temperature $T_N = 8$ K. An additional excitation with rather low intensity appears on the low-frequency side of mode 2. A closer inspection reveals that a third mode is hidden below the main resonance. This can best be seen by the slight differences of the measured reflectivity close to 370 cm^{-1}, at 9 and at 5 K. This evolution of a slight shoulder just below T_N could easily be analysed with the used fit routine and is indicated in figure 3. The overall splitting of mode 2 at low temperatures approximately amounts to 17 cm^{-1} (see frame (a) of figure 3). A splitting of mode 2, but only into two modes, has also been observed by Sushkov *et al* [13] in ZCO. In this compound a shoulder appears on the high-frequency side of the main intensity with an overall splitting of the order of 11 cm^{-1}. As documented in figure 4, in the magnetically ordered phase of CCO a small anomaly also becomes visible close to 500 cm^{-1}. In a first step, we assumed that this small dip corresponds to an additional weak phonon mode close to 500 cm^{-1}. But we were not able to describe the data with this assumption by using the fit routine, keeping all parameters of mode 3 constant and adding an additional mode with reasonable starting parameters. Finally we found out that the only way to consistently describe the experimental results is to assume a splitting of mode 3 into two almost equally strong modes by an amount of approximately 20 cm^{-1}. This of course means that both TO and LO modes

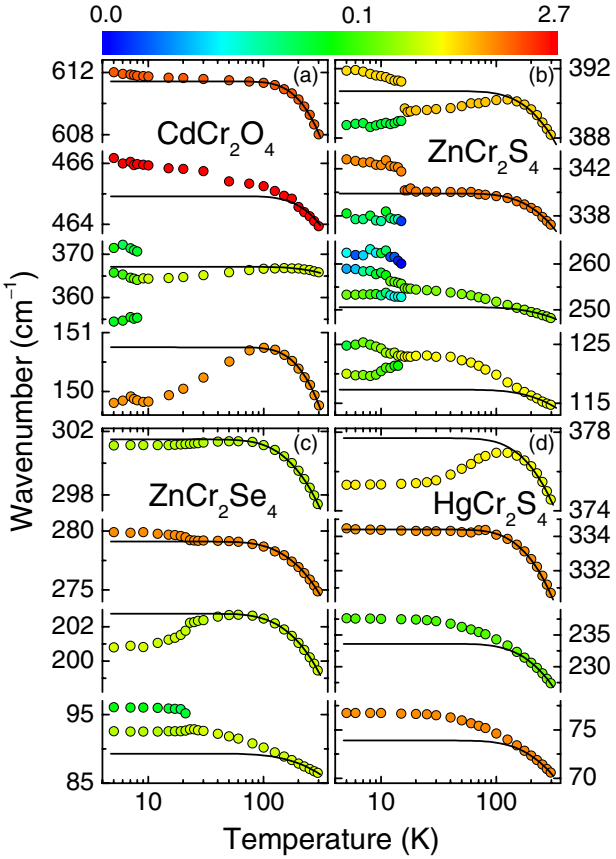

Figure 3. Temperature dependence of the phonon eigenfrequencies for $CdCr_2O_4$ (a) $ZnCr_2S_4$ (b) $ZnCr_2Se_4$ (c) and $HgCr_2S_4$ (d). The mode strength is indicated by a colour scale extending from 0.001 (dark blue) to 2.7 (bright red). Solid lines illustrate purely anharmonic behaviour.

are split by this amount. The splitting is of the same order of magnitude when compared to the over-all splitting of mode 2, which amounts to approximately 17 cm^{-1}. However, as these results did not follow from the analysis with the automated fit routine, but were derived by changing eigenfrequencies and damping by intuition and by trial and error, we did not include these results in figure 3.

As a splitting of all modes has been theoretically predicted by Fennie and Raabe [15], within a first principle model, as well as within LSDA + U (a local spin density approximation with a static mean-field approximation for the local Coulomb interaction U), we also checked the other modes. We found no indications of splitting, not even in the width parameter, for mode 4. Mode 1 reveals a slight increase in the width of the phonon excitation when entering the AFM phase, at least some hint for a possible hidden splitting below experimental resolution. Finally we made a closer inspection of the phonon modes of $ZnCr_2O_4$ at low temperatures. Modes 2 and 3 are shown in figure 5 on an enlarged scale for clarity. The splitting of mode 2 is fully compatible with the results of Sushkov *et al* [13]. But again we detected a small anomaly at 553 cm^{-1}, which evolves just at the AFM phase transition, very similar to the observations in $CdCr_2O_4$. The inset documents that this anomaly is just on the border of being detectable within our experimental accuracy, but probably signals a splitting of this mode, similar to the observations in CCO.

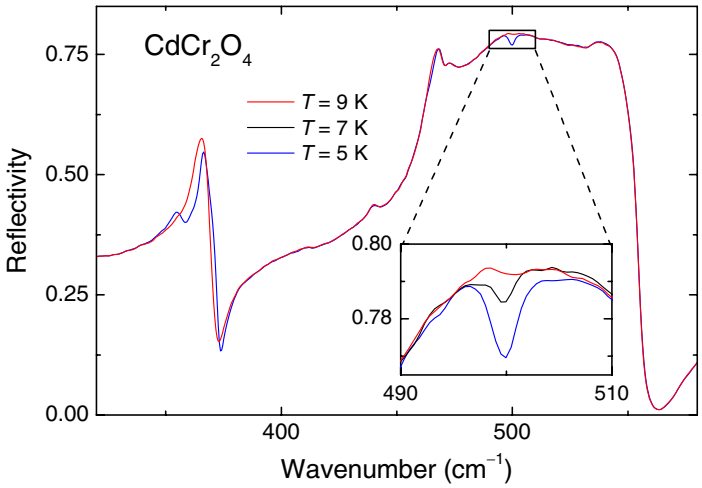

Figure 4. Enlarged scale for the reflectivity of $CdCr_2O_4$ for temperatures around the AFM ordering temperature $T_N = 8$ K. A clear splitting of mode 2 and a weak anomaly close to 500 cm^{-1} are observed. The latter can be modelled assuming a splitting of mode 3 into two modes of almost equal strength (see text).

Returning to figure 3, in ZCSe only the lowest-frequency mode (mode 1) exhibits a splitting [12]. In ZCS all modes are split [2]. Finally, despite the fact that HCS also undergoes AFM ordering below 23 K, no signature of split modes can be observed, and the phonon spectra in the antiferromagnetically ordered state look similar to those in FM $CdCr_2S_4$ [32].

In addition to the temperature dependence of the eigenfrequencies, figure 3 also indicates the strength of the modes as function of temperature. To get an estimate of the dielectric strength, $\Delta\epsilon$ has been calculated via

$$\Delta\epsilon_j = \epsilon_\infty \left(\frac{\omega_{\mathrm{L}j}^2 - \omega_{\mathrm{T}j}^2}{\omega_{\mathrm{T}j}^2} \right) \prod_{i=j+1} \frac{\omega_{\mathrm{L}i}^2}{\omega_{\mathrm{T}i}^2}, \tag{3}$$

which is indicated in figure 3 as a colour code, extending over three decades and running from 0.001 (dark blue for some of the low-intensity split modes) up to 2.7 (dark red, mainly for mode 3). In IR experiments the strength of a mode is directly related to the ionicity of a bond, or to the effective charges of the vibrating ions [32]. Mode 3 is rather strong in all compounds. It involves displacements of the Cr versus the X ions forming predominantly ionic bonds. It is also evident that the IR active phonons are intense in the oxide and weak in the selenide, indicating the decreasing electronegativity of the anions and consequently the increasing tendency for the formation of partly covalent bonds in the selenide.

In what follows, we would like to focus on the temperature dependence of the phonon eigenfrequencies: starting from high temperatures, the frequencies of the phonon modes increase as usually observed in anharmonic crystals. To get an estimate of this anharmonic contribution, the temperature dependence was fitted assuming

$$\omega_j = \omega_{0j} \left(1 - \frac{c_j}{\exp(T/\Theta) - 1} \right). \tag{4}$$

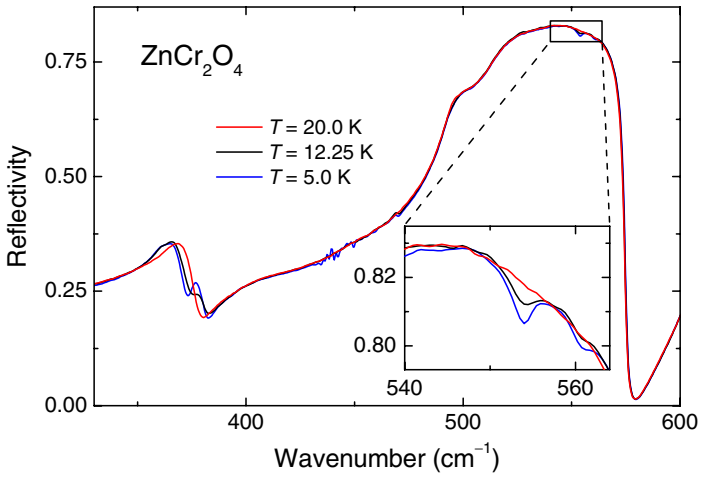

Figure 5. Partial view of the reflectivity spectra of $ZnCr_2O_4$ for temperatures close to the Néel temperature of $T_N = 12.5$ K. In addition to the clear splitting of mode 2 also mode 3 shows a temperature dependent anomaly at about 553 cm^{-1}, comparable to $CdCr_2O_4$.

Here ω_{0j} indicates the eigenfrequency of mode j at 0 K, c_j is a mode dependent scale factor of the anharmonic contributions and Θ denominates a rough estimate of the Debye temperature as determined from an average of the four IR active phonon frequencies. For the analysis the following Debye temperatures have been determined: CCO: $\Theta = 571$ K, ZCS: $\Theta = 392$ K, ZCSe: $\Theta = 309$ K, and HCS: $\Theta = 361$ K. The result of these fits to the high-temperature eigenfrequencies ($T > 100$ K) are indicated for all modes as solid lines in figure 3. It is clear that for $T < 100$ K all modes reveal significant deviations of the order of some percent from this purely anharmonic behaviour. In addition to these anomalies in the temperature dependence, some modes reveal a clear splitting below the corresponding AFM phase transitions.

The pattern of these splittings is very different for the different compounds. This has been outlined in detail by Tchernyshyov *et al* [10, 11] showing that the details of the particular Néel order will depend on the details of lattice distortions and bond order established by the spin-Teller effect. CCO is a geometrically frustrated magnet and undergoes AFM order into a spiral structure at 6 K. Here modes 2 and 3 split in the AFM phase. Mode 2 splits into three branches, while for mode 3 a small anomaly evolves at low temperatures, which can hardly be analysed (see figure 4). Figure 3 clearly documents that in ZCS, which is bond-frustrated [3] and reveals a complex collinear spin structure in the ground state, all phonon modes split. Finally, ZCSe and HCS, which undergo AFM phase transitions into spiral spin phases and are dominated by FM exchange, again behave differently: in ZCSe only mode 1 splits, a splitting which can be fully suppressed in an external magnetic field of 6 T [12]. HCS shows no splitting at all. Nevertheless, the eigenfrequencies reveal significant shifts when entering the AFM phases.

To analyse these temperature-induced shifts of the eigenfrequencies in more detail, we calculated the differences between measured frequencies and the calculated and extrapolated anharmonic behaviour (solid lines in figure 3). These differences for all modes are shown in figure 6. For mode 1 (figure 6(a)) the shifts in the almost FM sulfides and selenides are positive and amount to approximately 5 cm^{-1}. It is small and negative for geometrically frustrated CCO. A splitting can only be observed for ZCS and ZCSe and amounts to 5 and 3 cm^{-1}, respectively.

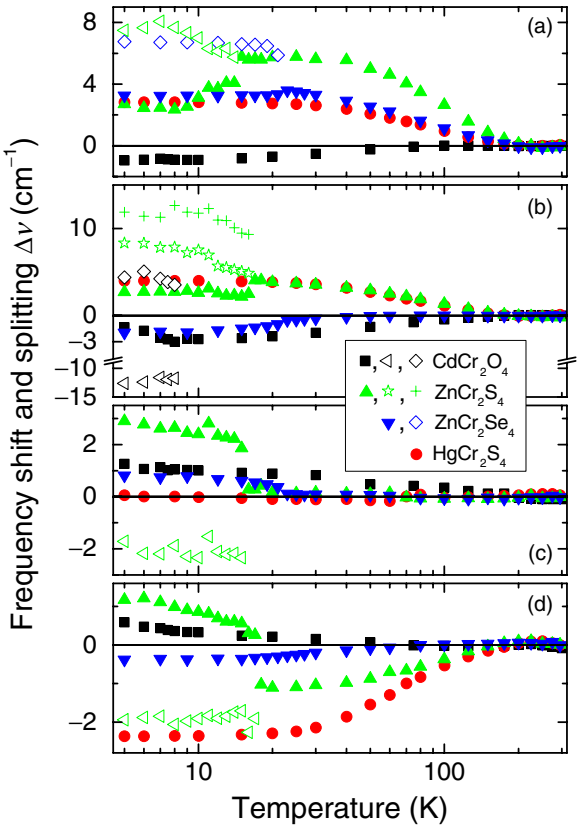

Figure 6. Temperature dependence of shift and splitting of all eigenfrequencies for $CdCr_2O_4$ (black symbols), $ZnCr_2S_4$ (green symbols), $ZnCr_2Se_4$ (blue symbols), and $HgCr_2S_4$ (red circles) for modes 1 (a), 2 (b), 3 (c), and for mode 4 (d).

For mode 2 (figure 6(b)), ZCS and HCS exhibit positive, CCO and ZCSe exhibit negative shifts. With the exception of almost FM HCS and ZCSe, the phonons for all other compounds split below T_N. For mode 3 (figure 6(c)) the shift for all compounds is small and positive. ZCS and CCO (not analysed) exhibit a splitting. Finally, mode 4 in HCS, ZCS and ZCSe shows negative shifts, while CCO has a small positive shift (figure 6(d)). Only ZCS exhibits a splitting of mode 4. It is interesting to note that specifically for HCS and ZCS, a strong influence of spin-phonon coupling on the eigenfrequencies can already be detected at 100 K, obviously determined by the strong FM spin fluctuations (see figure 1).

The results of figure 6 can be directly compared with theoretical models: the frequency shift corresponds to the spin-correlation function times a spin-phonon coupling constant λ [13, 15, 16, 33, 34]

$$\omega = \omega^0 + \lambda \langle S_i \cdot S_j \rangle. \tag{5}$$

Here ω corresponds to a renormalized phonon frequency, while ω^0 is the eigenfrequency in the absence of spin-phonon coupling. $\langle S_i \cdot S_j \rangle$ denotes a statistical average for adjacent spins [33].

Assuming typical values for EuO, Baltensperger and Helman [16] arrived at an estimate of -0.2% for an average frequency shift. From figure 6 we find that the shifts are of the order of

some cm^{-1} for most compounds, yielding relative shifts of some percent for the low-frequency modes and of less than 1% for the high-frequency modes. The splitting has been calculated for $ZnCr_2O_4$ by Fennie and Rabe from first principle methods. These authors find splittings of the order of 5–10 cm^{-1} for the low-frequency modes and of 2–3 cm^{-1} for the high frequency modes, which compare reasonably to our results.

Wakamura and Arai calculated the frequency shifts below T_C in FM $CdCr_2S_4$ and assumed negative contributions to the mode frequency from FM exchange and positive frequency shifts arising from AFM exchange. Below T_C, the authors experimentally found positive shifts for the low-frequency modes 1 and 2 and negative shifts for the high frequency modes 3 and 4. They concluded that the FM Cr–S–Cr bonds dominate modes 3 and 4, while the AFM linkage Cr–S–Cd–S–Cr determines the positive shifts of the eigenfrequencies of modes 1 and 2. Our experimental observations in almost FM $HgCr_2S_4$ are very similar, with large positive shifts for modes 1 and 2 and a negative shift for mode 4. The eigenfrequencies of mode 3 remain almost unshifted and reveal the normal anharmonic temperature dependence. These frequency shifts due to the spin-phonon coupling set in already at high temperatures, documenting that HCS is dominated by FM fluctuations. The onset of AFM order at 22 K gives no fingerprint in the temperature dependence of the eigenfrequencies. This pattern of frequency shifts is similar for most compounds shown in figure 6. HCS, ZCSe and ZCS exhibit a spiral spin order at low temperatures, which in the case of ZCS is followed by a mixed phase of spiral order coexisting with a complex collinear order. Only AFM geometrically frustrated CCO behaves differently with positive shifts of modes 3 and 4 and negative shifts of modes 1 and 2. And indeed, the magnetic order of CCO can best be described as a complex collinear state [21, 22].

4. Conclusions

The magnetic ions in chromium spinels (spin-only $S = 3/2$, no spin–orbit coupling) reside on a pyrochlore lattice, which in the case of next-nearest-neighbour AFM exchange is strongly frustrated. But in addition, depending on the size of the anions, FM and AFM exchange compete. It is this coexistence of geometrical frustration and bond frustration which constitutes a variety of complex ground states as a function of Cr–Cr separation or, as we have plotted in figure 1, as a function of CW temperatures. The frustration in all compounds, geometric as well as bond frustration, seems to be released by a spin-driven Jahn–Teller effect [9, 10, 12], inducing lattice anomalies and strong symmetry breaking in the dynamic variables.

In this report we presented a detailed study of the phonon properties in the PM and AFM states. We observed strong shifts of the eigenfrequencies and characteristic splittings of the phonon modes, which are different for the different order of the magnetic moments. Frequency shifts and mode splitting are compared for all compounds and are related to a spin-correlation function of nn spins. Moreover, the temperature dependence of the splittings and shifts seem to follow the sublattice magnetization in the ordered compounds. This seems to be best documented for $ZnCr_2S_4$, which shows a splitting of all modes below T_N (green symbols in figure 6 (a)–(d)). But for some modes, short-range order effects extending to temperatures far above T_N are clearly observed. Positive and negative shifts can be related to dominating FM and AFM exchange acting on specific bonds, which are actively involved in the IR active modes.

Finally, we also analysed the intensity of the different modes and found, as expected from simple electronegativity considerations, decreasing mode intensities when moving from the oxide over the sulfide to the selenides. These decreasing mode intensities signal an increasing covalency of the bonds, with $CdCr_2O_4$ being strongly ionic, while $ZnCr_2Se_4$ is predominantly covalent bonded.

Acknowledgments

This work was supported by the Collaborative Research Center SFB 484 (Augsburg). The support of US CRDF and MRDA via BGP III grant MP2-3050 is also gratefully acknowledged.

References

[1] Baltzer P K, Wojtowicz P J, Robbins M and Lopatin E 1966 *Phys. Rev.* **151** 367–77
[2] Hemberger J, Rudolf T, Krug von Nidda H-A, Mayr F, Pimenov A, Tsurkan V and Loidl A 2006 *Phys. Rev. Lett.* **97** 087204
[3] Lee S-H, Broholm C, Ratcliff W, Gasparovic G, Huang Q, Kim T H and Cheong S-W 2002 *Nature* **418** 856–8
[4] Hemberger J, Krug von Nidda H-A, Tsurkan V and Loidl A 2006 Colossal magnetostriction and negative thermal expansion in the frustrated antiferromagnet $ZnCr_2Se_4$ *Preprint* cond-mat/0607811
[5] Tsurkan V, Hemberger J, Krimmel A, Krug von Nidda H-A, Lunkenheimer P, Weber S, Zestrea V and Loidl A 2006 *Phys. Rev.* B **73** 224442
[6] Hemberger J, Lunkenheimer P, Fichtl R, Krug von Nidda H-A, Tsurkan V and Loidl A 2005 *Nature* **434** 364–7
[7] Weber S, Lunkenheimer P, Fichtl R, Hemberger J, Tsurkan V and Loidl A 2006 *Phys. Rev. Lett.* **96** 157202
[8] Kino Y and Lüthi B 1971 *Solid State Commun.* **9** 805–8
[9] Yamashita Y and Ueda K 2000 *Phys. Rev. Lett.* **85** 4960–3
[10] Tchernyshyov O, Moessner R and Sondhi S L 2002 *Phys. Rev. Lett.* **88** 067203
[11] Tchernyshyov O, Moessner R and Sondhi S L 2002 *Phys. Rev.* B **66** 064403
[12] Rudolf T, Kant Ch, Mayr F, Hemberger J, Tsurkan V and Loidl A 2007 *Phys. Rev.* B **75** 052410
[13] Sushkov A B, Tchernyshyov O, Ratcliff W II, Cheong S W and Drew H D 2005 *Phys. Rev. Lett.* **94** 137202
[14] Massidda S, Posternak M, Baldereschi A and Resta R 1999 *Phys. Rev. Lett.* **82** 430–3
[15] Fennie C J and Rabe K M 2006 *Phys. Rev. Lett.* **96** 205505
[16] Baltensperger W and Helman J S 1968 *Helv. Phys. Acta* **41** 668–73
[17] Baltensperger W 1970 *J. Appl. Phys.* **41** 1052–4
[18] Brüesch P and D'Ambrogio F 1972 *Phys. Status Solidi* b **50** 513–26
[19] Wessels A L, Czekalla R and Jeitschko W 1997 *Mater. Res. Bull.* **33** 95–101
[20] Ueda H, Mitamura H, Goto T and Ueda Y 2006 *Phys. Rev.* B **73** 094415
[21] Chern G-W, Fennie C J and Tchernyshyov O 2006 *Phys. Rev.* B **74** 060405(R)
[22] Chung J-H, Matsuda M, Lee S-H, Kakurai K, Ueda H, Sato T J, Takagi H, Hong K-P and Park S 2005 *Phys. Rev. Lett.* **95** 247204
[23] Hamedoun M, Wiedenmann A, Dormann J L, Nogues M and Rossat-Mignod J 1986 *J. Phys. C: Solid State Phys.* **19** 1783–800
[24] Plumier R 1965 *C. R. Acad. Sci. Paris* **260** 3348–50
[25] Plumier R 1966 *J. Phys.* **27** 213–9
[26] Akimitsu J, Siratori K, Shirane G, Iizumi M and Watanabe T 1978 *J. Phys. Soc. Japan* **44** 172–80
[27] Chapon L C, Radaelli P G, Hor Y S, Telling M T F and Mitchell J F 2006 Non-collinear long-range magnetic ordering in $HgCr_2S_4$ *Preprint* cond-mat/0608031

[28] Dwight K and Menyuk N 1967 *Phys. Rev.* **163** 435–43
[29] Lutz H D, Wäschenbach G, Kliche G and Haeuseler H 1983 *J. Solid State Chem.* **48** 196–208
[30] Zwinscher J and Lutz H D 1995 *J. Solid State Chem.* **118** 43–52
[31] Kuzmenko A 2006 RefFIT version 1.2.44, University of Geneva, online at http://optics.unige.ch/alexey/reffit.html
[32] Wakamura K and Arai T 1988 *J. Appl. Phys.* **63** 5824–9
[33] Lockwood D J and Cottam M G 1988 *J. Appl. Phys.* **64** 5876–8
[34] Wesselinowa J M and Apostolov A T 1996 *J. Phys.: Condens. Matter* **8** 473–88